

# Some manifestations of two-component dark matter structure in vectorlike hypercolor model

M Bezuglov<sup>1,3</sup>, V Beylin<sup>2</sup>, V Kuksa<sup>2</sup>

<sup>1</sup> Bogoliubov Laboratory of Theoretical Physics, Joint Institute for Nuclear Research, Joliot-Curie 6, 141980 Dubna, Moscow region, Russia

<sup>2</sup> Theoretical Physics Department, Southern Federal University, 344090 Stachki av. 194, Rostov-on-Don, Russia

<sup>3</sup> Moscow Institute of Physics and Technology (State University), 9 Institutskiy per., 141701 Dolgoprudny, Moscow Region, Russian Federation

E-mail: bezuglov.ma@phystech.edu

**Abstract.** In the framework of vectorlike hypercolor model with two generations it have been considered some peculiarities of diffuse gamma spectrum which is produced in the process of the Dark Matter annihilation. The model suggests two Dark Matter candidates and both of them contribute to this cross section depending on the model parameters. Masses of these DM components are estimated from analysis of kinetics of the DM and data on relic abundance.

## 1. Introduction

In accordance with modern astrophysical data, approximately a quarter of the mass of the Universe is so-called dark matter (DM) consisting of weakly interacting mass particles (WIMPS) of unknown nature; they can be elementary particles or some compound objects like e.g. "dark atoms". Independently on the DM candidates origin, the thermal freeze-out model assumes that when the particles concentration becomes too small to actively annihilate, (due to the Universe expansion) the co-moving density of the DM "freezes" and remains nearly constant since then. So, the relic abundance is determined by the DM particles annihilation cross section which depends, in turn, on peculiarities of the underlying model i.e. on mass, structure and interactions of these particles.

Hopes for direct observations of the DM candidates are now not so optimistic as it was before the LHC began to operate. As the SUSY scale and corresponding DM candidates (neutralino in all possible -ino combinations) have been shifted to larger energy scale, the search of the DM manifestations is concentrated more at using of indirect detection methods. Characteristic value of  $\langle \sigma_{ann} v \rangle = O(1)$  pb which can be extracted from the data on the relic DM density is specific for the Standard Model (SM) energetic scale. Then, we can expect that the interval of the DM particles masses should be  $\sim (10^1 - 10^4)$  GeV.

The search for the DM carriers with these masses at the colliders continues, but in indirect way for studying the DM candidates are becoming increasingly important[1,2,3,4,5]. In particular, the investigation of many astrophysical phenomena and the signals generated by them is currently one of the main tools for analyzing the DM structure, properties and distribution in the Galaxy. Along with the analysis of the energy spectra and angular distributions of cosmic



Content from this work may be used under the terms of the [Creative Commons Attribution 3.0 licence](#). Any further distribution of this work must maintain attribution to the author(s) and the title of the work, journal citation and DOI.

rays, of particular interest are the observational data and the results of studying the spectra of photons of both galactic and extragalactic origin [6,7,8]

Using available data on the distribution of supernova remnants and blazars in the Galaxy, as well as approximate maps of magnetic fields near these objects and the center of the Galaxy, the differential fluxes of both cosmic rays and photons and neutrinos can be measured by space telescopes and simulated in the frameworks of different models.

These considerations are based on recent astrophysical data and hypotheses, and also used concepts of the DM nature and origin that do not contradict astrophysical and collider measurements. Namely, the options proposed by the various inevitable extensions of the Standard Model (SM) give possibility to analyze results of observations and predict some astrophysical manifestations of the DM particles. The using of cosmic gamma-ray data is an important and unique instrument to get information on the matter distribution and its interactions in our Galaxy and beyond. So, we should work in the framework of some reasonable model of the SM extension offering the DM candidates in accordance with known data of experiments and observations.

In this paper, we consider the SM extended by adding of a minimal sector of heavy fermions — hyper-quarks (H-quarks) in confinement [9,10,11,12,13]. Further, the  $\sigma$ - model allows to describe the phenomenology of di-H-quarks and pseudo-Nambu-Goldstone (pNG) state connected with different H-quark currents. H-color model contains two neutral particles which can be interpreted as the DM components. The minimal version of the SM extension contains two H-quarks generations and two hypercolors,  $N_{HC} = 2$ . In [10,11] weak interaction couplings constructing is described with the standard-like chiral asymmetric set of new fermion doublets having a nonzero hypercharge. An important distinction from the “standard” Technicolor is that two left doublets of H-quarks can be transformed into one doublet of Dirac H-quarks with vectorlike weak interaction. Hypercharges of H-quark generations are opposite providing the absence of anomalies in the model. In the one loop, H-quarks are degenerated,  $M_U = M_D$ . Here  $U, D$  are H-quark fields, their electric charges are  $q_U = q_D = -1/2$  in accordance with zero hypercharge,  $Y = 0$ . Dirac states which correspond to constituent quarks occur by the using of a scalar field (hyper- $\sigma$ - meson) with non-zero vacuum expectation value; is arises as a scalar singlet pseudo-Nambu-Goldstone (pNG) boson in the framework of the simplest linear  $\sigma$ - model. Then, structure of the pNG multiplet is defined by the global symmetry breaking  $SU(4) \rightarrow Sp(4)$ . The model Lagrangian has a global  $U_{HB}(1)$  symmetry providing the lightest neutral H-baryon/H-diquark states ( $B^0, \bar{B}^0$ ) stability. These states possess an additive conserved H-baryon number. At the same time, the Lagrangian conserves a multiplicative quantum number — the modified charge conjugation parity (hyper-G or HG-parity). As a consequence, the lightest neutral H-pion state is stable [14,11].

Complete set of the lightest spin-0 H-hadrons in the model includes pNG states (pseudoscalar H-pions  $\tilde{\pi}_k$  and scalar complex H-diquarks/H-baryons  $B^0$ ), their opposite-parity partners  $\tilde{a}_k$  and  $A^0$ , and singlet H-mesons  $\tilde{\sigma}$  and  $\tilde{\eta}$ . These states correspond to H-quark currents with different quantum numbers, H-baryons have not intrinsic  $C$ - and  $HG$ -parities, because of the charge conjugation reverses the sign of the H-baryon number. The model suggested contains also the elementary Higgs field which is not a pNG state.

Now, we can interpret neutral pNG particles,  $\tilde{\pi}^0$  and  $B^0$ , as the DM candidates (see also [12,15,16,17]). All necessary for the numerical analysis parts of the Lagrangian can be found in [11] describing H-quark interactions with the EW bosons as vectorlike. Note, direct interaction of  $B^0$  states with standard weak bosons is absent at one loop level, and fields  $\tilde{\sigma}, \tilde{\pi}, H$  ( $H$  is the standard Higgs boson field) interact with the H-quarks. Importantly, scalars H-sigma and Higgs boson mix with each other forming physical states,  $\theta$  is the angle of mixing which controls agreement of the model predictions with the SM precision data. Small  $s_\theta = \sin \theta \leq 0.1$  result to small values of corresponding parameters of Peskin-Tackeuchi[9,10]. Then, to analyze

quantitatively some processes with stable the DM candidates, we need in a few parameters only: tree-level masses of the DM components (H-pion and H-baryon), mass and v.e.v. of  $\tilde{\sigma}$ - meson. It is important, all restrictions on the oblique corrections are fulfilled in this variant of hypercolor [9,10]. In the scenario with a non-zero hypercharge and  $H - \tilde{\sigma}$  mixing a constraint for the  $T$  parameter value emerges [9,15]. Constraints on value of  $\theta$  follow from analysis of Peskin-Tackeuchi (PT) parameters. It has been found that  $\sin \theta \leq 0.1$  [9] to get away the problems with PT parameters and the measured characteristics of the SM Higgs boson. Then, to analyze quantitatively processes involving the DM particles, it is necessary to know only a few parameters: tree-level masses of the DM components (H-pion and H-baryon), mass and v.e.v. of  $\tilde{\sigma}$ - meson. The neutral component of the H-pion triplet,  $\tilde{\pi}^0$ , is the lightest, mass difference in the triplet results from electroweak loops only and is well known [12,17]:  $\Delta M_{\tilde{\pi}^0} = m_{\tilde{\pi}^\pm} - m_{\tilde{\pi}^0} \approx 0.16$  GeV. So, charged H-pion states can decay producing neutral H-pions (more detail can be found in [11]. Non-zero mass splitting in the H-pion triplet violates isotopic invariance, however,  $HG$ -parity corresponds to a discrete symmetry and the neutral H-pion remains stable independently on higher order corrections. Tree level masses of  $\tilde{\pi}^0$  and  $B^0$  are equal, and the mass splitting  $\Delta M_{B\tilde{\pi}} = m_{B^0} - m_{\tilde{\pi}^0}$  is defined only by electroweak diagrams due to mutual cancellation of all other contributions. Then, we get :

$$\Delta M_{B\tilde{\pi}} = \frac{-g_2^2 m_{\tilde{\pi}}}{16\pi^2} \left[ 8\beta^2 - 1 - (4\beta^2 - 1) \ln \frac{m_{\tilde{\pi}}^2}{\mu^2} + 2 \frac{M_W^2}{m_{\tilde{\pi}}^2} \left( \ln \frac{M_W^2}{\mu^2} - \beta^2 \ln \frac{M_W^2}{m_{\tilde{\pi}}^2} \right) - 8 \frac{M_W}{m_{\tilde{\pi}}} \beta^3 \left( \arctan \frac{M_W}{2m_{\tilde{\pi}}\beta} + \arctan \frac{2m_{\tilde{\pi}}^2 - M_W^2}{2m_{\tilde{\pi}}M_W\beta} \right) \right], \quad (1)$$

where  $\beta = \sqrt{1 - \frac{M_W^2}{4m_{\tilde{\pi}}^2}}$ . Dependence of  $\Delta M_{B\tilde{\pi}}$  on a renormalization point is a consequence of coupling of these pNG states with different H-quark currents i.e. possible components of the DM are generated by different structures. Then, we need to take into account the dependence of the DM measurable parameters on the renormalization parameter value.

We also suppose that other (not pNG) possible H-hadrons (including vector H-mesons) are heavier than the pNG bosons. In other words, the scale of explicit  $SU(4)$  symmetry breaking is small in comparison with the scale of the dynamical symmetry breaking. It is an analogy with the QCD, where the scale of chiral symmetry breaking is much larger than the masses of light quarks. Further, in order to satisfy the collider restrictions for new particles, we assume the masses of low-lying H-states are of the order of  $10^3$  GeV.

Now we can consider some features of the two-component Dark Matter in more detail. Namely, for neutral H-baryon states,  $B^0$ ,  $\bar{B}^0$ , and two charged H-pions together with the neutral one, the system of five Boltzmann kinetic equations should be solved. Charged H-pions are considered because in the triplet mass splitting is small and the it is necessary to take into account coannihilation processes at the early stage of the DM evolution[18].

For the analysis of DM kinetics it should be considered five basic Boltzmann kinetic equations for two states of the neutral H-baryon,  $B^0$ ,  $\bar{B}^0$  and two charged H-pions together with the neutral one. The reason is that the mass splitting in the triplet of H-pions is very small, so the processes of co-annihilation [18] contribute significantly to the annihilation cross section. Numerically, it has been shown in another vectorlike scenario in [17].

So, we have the following the system of equations (2)-(3), one for each DM component( $i, j = \tilde{\pi}^+, \tilde{\pi}^-, \tilde{\pi}^0; \mu, \nu = B, \bar{B}$ ):

$$\frac{da^3 n_i}{a^3 dt} = - \sum_j \langle \sigma v \rangle_{ij} (n_i n_j - n_i^{eq} n_j^{eq}) - \sum_j \Gamma_{ij} (n_i - n_i^{eq}) -$$

$$\sum_{j,\mu,\nu} <\sigma v>_{ij \rightarrow \mu\nu} \left( n_i n_j - \frac{n_i^{eq} n_j^{eq}}{n_\mu^{eq} n_\nu^{eq}} n_\mu n_\nu \right) + \\ \sum_{j,\mu,\nu} <\sigma v>_{\mu\nu \rightarrow ij} \left( n_\mu n_\nu - \frac{n_\mu^{eq} n_\nu^{eq}}{n_i^{eq} n_j^{eq}} n_i n_j \right). \quad (2)$$

We also get:

$$\frac{da^3 n_\mu}{a^3 dt} = - \sum_\nu <\sigma v>_{\mu\nu} \left( n_\mu n_\nu - n_\mu^{eq} n_\nu^{eq} \right) + \\ \sum_{\nu,i,j} <\sigma v>_{ij \rightarrow \mu\nu} \left( n_i n_j - \frac{n_i^{eq} n_j^{eq}}{n_\mu^{eq} n_\nu^{eq}} n_\mu n_\nu \right) - \\ \sum_{\nu,i,j} <\sigma v>_{\mu\nu \rightarrow ij} \left( n_\mu n_\nu - \frac{n_\mu^{eq} n_\nu^{eq}}{n_i^{eq} n_j^{eq}} n_i n_j \right), \quad (3)$$

where:

$$<\sigma v>_{ij} = <\sigma v> (ij \rightarrow XX) \\ <\sigma v>_{ij \rightarrow \mu\nu} = <\sigma v> (ij \rightarrow \mu\nu) \\ \Gamma_{ij} = \Gamma(i \rightarrow j XX), \quad (4)$$

and analogously for  $\mu$  and  $\nu$  components.

Charged H-pions eventually decay into  $\tilde{\pi}^0$ , so total densities of  $\tilde{\pi}$ ,  $B^0$  and  $\bar{B}^0$ , i.e.  $n_{\tilde{\pi}} = \sum_i n_i$  and  $n_B = \sum_\mu n_\mu$  are the main parameters. Introducing an equilibrium particle density,  $n_{eq}$ , for co-annihilation we use  $n_i/n \approx n_i^{eq}/n^{eq}$ . Further, because of  $m_{\tilde{\pi}}/M_B \approx 1$ , we get  $n_B^{eq}/n_{\tilde{\pi}}^{eq} = 2/3$  and the system is obviously simplified. The next step is to consider of small mass splitting between H-pions and  $B^0$ :  $\Delta M_{B^0 \tilde{\pi}^0}/m_{\tilde{\pi}^0} \leq 0.02$ ; now, the cross sections  $<\sigma v>_{\tilde{\pi}\tilde{\pi}}$  and  $<\sigma v>_{BB}$  are calculated with an account of the temperature dependence [18]. Denoting  $Y = n/s$  and  $x = m_{\tilde{\pi}}/T$ , where  $s$  is the entropy density, we get:

$$\frac{dY_{\tilde{\pi}}}{dx} = g(x, T) \left[ \lambda_{\tilde{\pi}} ((Y_{\tilde{\pi}}^{eq})^2 - Y_{\tilde{\pi}}^2) - \lambda_{\tilde{\pi}\tilde{\pi}} \left( Y_{\tilde{\pi}}^2 - \frac{9}{4} Y_B^2 \right) + \lambda_{BB} \left( Y_B^2 - \frac{4}{9} Y_{\tilde{\pi}}^2 \right) \right], \quad (5)$$

$$\frac{dY_B}{dx} = g(x, T) \left[ \lambda_B ((Y_B^{eq})^2 - Y_B^2) + \lambda_{\tilde{\pi}\tilde{\pi}} \left( Y_{\tilde{\pi}}^2 - \frac{9}{4} Y_B^2 \right) - \lambda_{BB} \left( Y_B^2 - \frac{4}{9} Y_{\tilde{\pi}}^2 \right) \right], \quad (6)$$

where  $g(x, T) = \frac{\sqrt{g(T)}}{x^2} \left\{ 1 + \frac{1}{3} \frac{d(\log g(T))}{d(\log T)} \right\}$ . Here, we use notations from [19]:  $\lambda_i = 2.76 \times 10^{35} m_{\tilde{\pi}} <\sigma v>_i$  ( $m$  is in GeV and  $<\sigma v>$  in  $\text{cm}^3 \text{s}^{-1}$ ) and  $Y_{\tilde{\pi}}^{eq} = 0.145(3/g(T))x^{3/2}e^{-x}$ ,  $Y_B^{eq} = 0.145(2/g(T))x^{3/2}e^{-x}$ ,  $g(T)$  is the number of relativistic degrees of freedom contributing to the energy density which can be estimated as  $g(T) \approx 100$ .

The DM present relic density  $\Omega h^2$  can be written in terms of the relic abundance  $\rho$  and critical mass density  $\rho_{crit}$ :

$$\Omega h^2 = \frac{\rho}{\rho_{crit}} h^2 = \frac{m s_0 Y_0}{\rho_{crit}} h^2 \simeq 0.3 \times 10^9 \frac{m}{\text{GeV}} Y_0. \quad (7)$$

Subscript "0" denotes quantities whose values are evaluated at present time.

Further, numerical solutions of the equations (5), (6) are presented as the set of regions in the plane of H-pion and H-sigma masses. (Relation between these masses is defined by the mixing

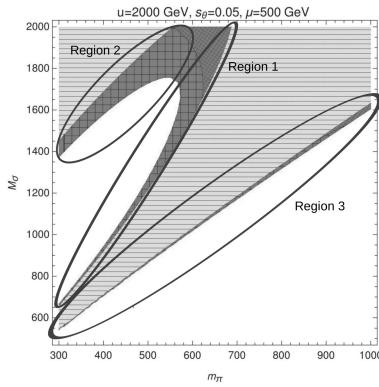


**Figure 1.** Numerical solution of the kinetic equations system in a phase diagram in terms of  $M_{\tilde{\sigma}}$  and  $m_{\tilde{\pi}}$  parameters; types of hatching are indicated in the text.

angle  $\theta$ , renormalization scale  $\mu$  and also by the vacuum parameter  $u$ .) Physically interesting areas are indicated by different hatching: vertical cells denote areas where we have correct DM relic density, here H-pions fraction is less than 25 percents ( $0.1047 \leq \Omega h_{HP}^2 + \Omega h_{HB}^2 \leq 0.1228$  and  $\Omega h_{HP}^2/(\Omega h_{HP}^2 + \Omega h_{HB}^2) \leq 0.25$ ); the hatching with oblique cells indicates domains where all parameters are the same, but H-pions make up just over a quarter of the DM ( $0.1047 \leq \Omega h_{HP}^2 + \Omega h_{HB}^2 \leq 0.1228$  and  $0.25 \leq \Omega h_{HP}^2/(\Omega h_{HP}^2 + \Omega h_{HB}^2) \leq 0.4$ ). Importantly, in all areas H-pion component can not dominate in the DM because of H-pions have tree level interactions with weak vector bosons.  $B^0$  component interacts with EW bosons only via H-quark and H-pion loops. The horizontal lines denote areas corresponding to permitted regions ( $\Omega h_{HP}^2 + \Omega h_{HB}^2 \leq 0.1047$ ), here the DM relic is not explained by H-color components only. Regions that are hatched with vertical lines are forbidden by direct experiments of the XENON collaboration (see also [20,21]). So, as it can be seen in figure 1, there are three areas where the recent DM density can be explained by the H-color model:

**Region 1:**  $M_{\tilde{\sigma}} > 2m_{\tilde{\pi}^0}$  and  $u \geq M_{\tilde{\sigma}}$ . We have small mixing, large masses of H-pions and, possibly, a significant fraction of H-pions.

**Region 2:** There is the same relation between  $M_{\tilde{\sigma}}$ ,  $m_{\tilde{\pi}^0}$ ,  $u$ , H-pion mass is smaller,  $m_{\tilde{\pi}} \approx 300 - 600$  GeV, and H-pion fraction is small.

**Region 3:**  $M_{\tilde{\sigma}} < 2m_{\tilde{\pi}}$ . This region is always possible, process  $\tilde{\sigma} \rightarrow \tilde{\pi}\tilde{\pi}$  is absent here; H-pion fraction in the DM relic can be large if the mass  $m_{\tilde{\pi}^0}$  is large and the mixing angle is small.

Thus, some intervals of possible values of masses are found and we use them to calculate cross sections of processes of type  $DM + DM \rightarrow X + Y + \gamma$ .

## 2. Diffuse photon emission as a probe of the DM annihilation

Now, we consider all channels of the DM particles annihilation into charged secondaries, corresponding diagrams are depicted in figure 2. Evidently, photons can be emitted from different lines, but virtual internal bremsstrahlung (VIB) processes follow from diagrams (g) and (h) only. These contributions indicate that there are some features of the DM candidates [6,22] defining by the interaction structure and by the origin of the DM particles.

Taking into account the ratio of H-pions to H-baryons, the full spectrum will be written as

$$\frac{d(\sigma v)}{dE_\gamma} E_\gamma^2 = \kappa^2 \frac{d(\sigma v_{\tilde{\pi}^0 \tilde{\pi}^0})}{dE_\gamma} E_\gamma^2 + (1 - \kappa)^2 \frac{d(\sigma v_{B^0 \bar{B}^0})}{dE_\gamma} E_\gamma^2, \quad (8)$$

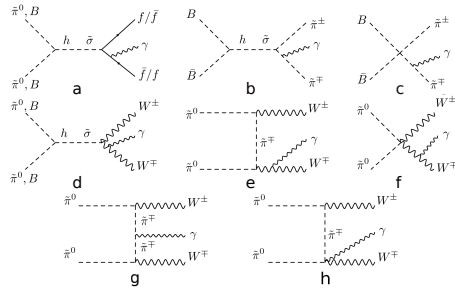


**Figure 2.** All necessary diagrams for processes with bremsstrahlung photons at tree level

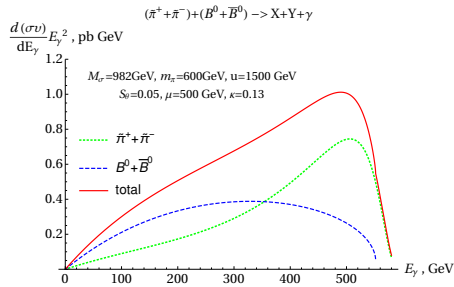


**Figure 3.** Photon spectrum for  $m_\pi = 600 \text{ GeV}$ ,  $M_\sigma$  is light.

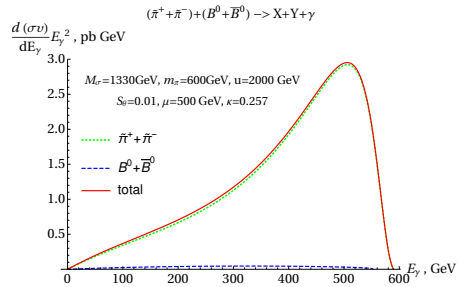


**Figure 4.** Photon spectrum for  $m_\pi = 600 \text{ GeV}$ ,  $M_\sigma$  is heavy.

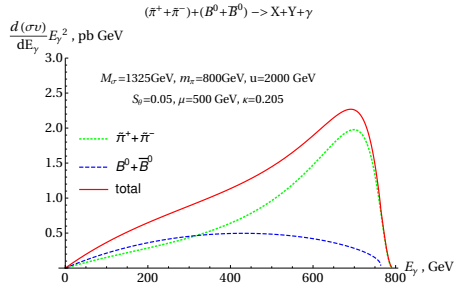


**Figure 5.** Photon spectrum for  $m_\pi = 800 \text{ GeV}$ ,  $M_\sigma$  is light.

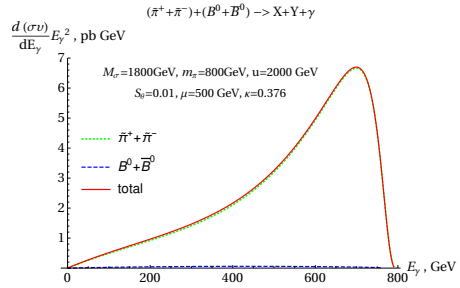


**Figure 6.** Photon spectrum for  $m_\pi = 800 \text{ GeV}$ ,  $M_\sigma$  is heavy.

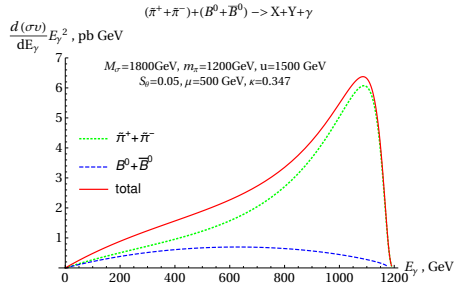


**Figure 7.** Photon spectrum for  $m_\pi = 1200 \text{ GeV}$ ,  $M_\sigma$  is light.

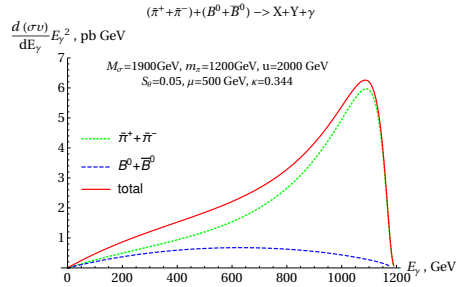


**Figure 8.** Photon spectrum for  $m_\pi = 1200 \text{ GeV}$ ,  $M_\sigma$  is heavier.

here fraction of H-pions is defined as:

$$\kappa = \frac{\Omega h_{HP}^2}{\Omega h_{HP}^2 + \Omega h_{HB}^2} \quad (9)$$

Therefore, it makes sense to follow the contributions to the total annihilation cross section from various DM components. A comparison of these values shows how the intensities of the photon signals from the annihilation of various DM parts differ. Immediately, we note that quantitatively main contributions come from processes with finite W-bosons, so annihilation of H-pions contributes mostly. The reason is obvious: H-baryons do not interact with EW bosons at the tree level. However, as it is seen from figures 3–8, there are some regions of the model parameters where the contribution from  $B^0$ – states annihilation is significant. We also found that the mass of  $\sigma$ – mesons is an important parameter since its variation can change the cross section value from  $-10\%$  to  $+50\%$ , approximately. This effect depends also on the mass of the DM component and it is seen better for the mass near 800 GeV. In this case, however, contribution from  $B^0$  is not large, it can be more substantial for lower mass  $\approx 600$  GeV. Thus, the relative contributions to the gamma flux intensity from annihilations of different DM components corresponds to the model content and depends on the structure of interactions.

### 3. Conclusion

The cross section calculated is a necessary element of analysis of the total diffuse photon flux. This consideration also makes it possible to separate contribution of VIB subprocesses which is an important part of the cross section, its value being  $\sim 30\%$ . Another interesting feature is the shape of the photon spectrum which is defined by the presence of two components in the DM. This structure stands out better or worse depending on the relative contribution of the components, as well as on the values of model parameters.

Photon signals from annihilation of the DM clumps should be substantially larger because of high density of interacting particles [23]. We suggest that not only monochromatic but also photon internal bremsstrahlung and VIB are an important probe of the DM distribution and dynamics.

### Acknowledgments

We thank V. Korchagin, N. Volchanskiy and M. Khlopov for helpful discussions and comments. This work is supported by Russian Scientific Foundation (RSCF) Grant N 18-12-00213.

### References

- [1] Hooper D 2007 Indirect searches for dark matter (signals, hints and otherwise) *Preprint* arXiv:0710.2062
- [2] Bringmann T, Weniger C 2012 Gamma ray signals from dark matter: Concepts, status and prospects *Dark Universe* **1** 194
- [3] Cirelli M 2012 Indirect searches for dark matter: a status review *Preprint* arXiv:1202.1454v5
- [4] Funk S 2013 Indirect detection of dark matter with rays *Preprint* arXiv: 1310.2695
- [5] Duerr M, Perez P F and Smirnov J 2016 Scalar dark matter: direct vs. indirect detection *J. High Energy Phys.* JHEP06(2016)152
- [6] Bringmann T, Bergstrom L and Edsjo J 2008 New gamma-ray contributions to supersymmetric dark matter annihilation *J. High Energy Phys.* JHEP0801(2008)049
- [7] Zavala J, Springel V and Boylan-Kolchini M 2010 Extragalactic gamma-ray background radiation from dark matter annihilation *MNRAS* **405**(1) 593–612
- [8] Hutten M, Combet C and Maurin D 2017 Extragalactic diffuse gamma-rays from dark matter annihilation: revised prediction and full modelling uncertainties *Preprint* arXiv:1711.08323
- [9] Pasechnik R, Beylin V, Kuksa V and Vereshkov G 2013 *Phys. Rev. D* **88** 075009
- [10] Beylin V A, Vereshkov G M, Kuksa V I 2016 *Phys. Part. Nucl. Lett.* **13** 1
- [11] Beylin V, Bezuglov M, Kuksa V and Volchanskiy N 2017 *Adv. in HEP.* **2017**, 1765340
- [12] Ryttov T A, Sannino F 2008 *Phys. Rev. D* **78** 115010

- [13] Kilic C, Okui T, Sundrum R 2010 The LHC Phenomenology of vectorlike confinement *JHEP* **04** 128
- [14] Bai Y and Hill R J 2010 *Phys. Rev. D* **82** 111701
- [15] Pasechnik R, Beylin V, Kuksa V, Vereshkov G 2013 *Eur. Phys. J. C* **74** 08
- [16] Pasechnik R, Beylin V, Kuksa V, Vereshkov G 2016 *Int. J. Mod. Phys. A* **31** 1650036
- [17] Beylin V, Bezuglov M and Kuksa V 2017 *Int. J. Mod. Phys. A* **32** 1750042
- [18] Griest K and Seckel D 1991 *Phys. Lett. B* **43** 3191
- [19] Steigman G, Dasgupta B and Beacom J F 2012 *Phys. Lett. B* **86** 023506
- [20] Aprile E *et al.* (XENON Collaboration) 2017 *Phys. Rev. Lett.* **119** 181301
- [21] Aalbers J *et al.* (DARWIN Collaboration) 2016 DARWIN: towards the ultimate dark matter detector *JCAP* **1611** 017
- [22] Garny M, Ibarra A, Pato M and Vogl S 2013 Internal bremsstrahlung signatures in light of direct dark matter searches *JCAP* **12** 046
- [23] Belotsky K, Kirillov A and Khlopov M 2012 Gamma-ray evidences of the dark matter clumps *Preprint* arXiv:1212.6087